Sorption of ^{89}Zr on hydroxyapatite nanoparticles as carriers for nuclear medicine

Andrey G. Kazakov & Alexander V. Severin

Journal of Radioanalytical and Nuclear Chemistry
An International Journal Dealing with All Aspects and Applications of Nuclear Chemistry

ISSN 0236-5731

J Radioanal Nucl Chem
DOI 10.1007/s10967-020-07192-8

Springer

Journal of Radioanalytical and Nuclear Chemistry
https://doi.org/10.1007/s10967-020-07192-8

Sorption of ^{89}Zr on hydroxyapatite nanoparticles as carriers for nuclear medicine

Andrey G. Kazakov[1,2] · **Alexander V. Severin**[2]

Received: 21 February 2020

Abstract
The sorption behavior of ^{89}Zr on hydroxyapatite ($Ca_{10}(PO_4)_5(OH)_2$, HA) nanoparticles in an aqueous medium and 0.9% NaCl at various pH values was studied. The fast kinetics of the process was determined; the stability of the obtained conjugate in a model biological medium at 25 and 37 °C was shown. The possibility of further use of the ^{89}Zr@HA conjugate in various radiopharmaceuticals is discussed.

Keywords ^{89}Zr · Hydroxyapatite · Nuclear medicine · Nanoparticles as carriers · Radiopharmaceuticals · Sorption

Introduction

^{89}Zr is one of the most attractive radionuclides for positron emission tomography due to its nuclear physical characteristics [1]. It can be easily produced on natural monoisotopic yttrium by reactions ^{89}Y(p,n)^{89}Zr and ^{89}Y(d,2n)^{89}Zr [2, 3], having a high yield and maximum cross-sections at energies of just over 10 MeV [4, 5]. The literature describes the separation of ^{89}Zr from irradiated yttrium targets by extraction methods [6–8], ion-exchange and extraction chromatography [9–15].

The studied radiopharmaceuticals based on ^{89}Zr can be divided into two groups: the first, where ^{89}Zr is chelated by various complexes and then bound to antibodies, and the second, where various nanoparticles act as ^{89}Zr carriers. In the first case, the coordination chemistry of zirconium creates some difficulties with chelation. Strong bonding of zirconium requires 8 electron-donating atoms around it [16] leading to problems when using chelators typical of nuclear medicine. For example, the ^{89}Zr complex with deferroxamine (DFO) is partially unstable in the body [17], and the chelators DTPA (diethylenetriaminepentaacetic acid) and DOTA (1,4,7,10-tetraazocyclododecane-1,4,7,10-tetraacetic acid) have binding problems [18, 19]. For this reason, much attention of scientists today is devoted to the search for new promising chelators [19–22]. In the second case, various biocompatible nanoparticles are investigated for ^{89}Zr delivery: high density lipoprotein [23], liposomal nanoparticles [24, 25], gold nanoparticles [26], quantum dots [27] and nanodots [28].

This work is devoted to the study of hydroxyapatite nanoparticles (HA, $Ca_{10}(PO_4)_6(OH)_2$), which are non-toxic, biocompatible, biodegradable etc. [29] as a carriers of ^{89}Zr in radiopharmaceuticals. HA and its derivatives have long been actively investigated for its using as carriers of medical radionuclides and is considered as a platform for both therapeutic (^{177}Lu [30, 31], ^{153}Sm [32], ^{223}Ra [33], ^{211}Pb [34]) and diagnostic radionuclides (^{67}Zn [35], ^{64}Cu [36], ^{89}Zr [37]). Thus, high stability of ^{177}Lu-labeled HA in vitro has been demonstrated [30] and the possibility of successful use of ready-to-use kits with such particles in clinical trials in patients with rheumatoid arthritis was also shown [31]. The biodistribution of ^{153}Sm-labeled HA in the human body was studied, and HA particles were found to be potentially useful radiation synovectomy agent [32]. The sorption behavior of α-emitter ^{223}Ra on HA was studied in vitro, and the high stability of the obtained conjugates in various media was determined [33], which make possible to consider HA as a promising carrier to ^{223}Ra in nuclear medicine. The possibility of sorption and cocrystallization binding of lead with HA acting as a potential carrier of short-lived medicine isotopes ^{211,212}Pb was shown in [34]. Sorption of copper and zinc ions

✉ Andrey G. Kazakov
adeptak92@mail.ru

[1] Vernadsky Institute of Geochemistry and Analytical Chemistry of the Russian Academy of Sciences, Kosygin St., 19, Moscow, Russia 119991

[2] Chemistry Department, Lomonosov Moscow State University, Leninskie Gory, 1, Moscow, Russia 119991

Published online: 05 May 2020

on HA was studied in vitro, and it was shown that HA can become a platform for drugs with medical isotopes ^{69m}Zn and ^{64}Cu [35, 36].

Earlier, we developed an approach in which 2 variants of isotope binding to HA are possible: co-crystallization and sorption. For example, it was shown for ^{69m}Zn that both variants lead to a uniform distribution of the cation over the surface of the nanocrystal [38]. At the same time, using of co-crystallization method of binding could change the morphology and structure of the carrier [34, 36]. In this work, we develop and optimize precisely the sorption method of binding the ^{89}Zr to HA, in which the doping cation minimally affects the structure and morphology of the support.

In our recent work, we also investigated the possible mechanism of ^{89}Zr sorption on HA by studying the surface of HA with stable zirconium adsorbed on it by XPS method [37]. This work is devoted to the search for optimal conditions for ^{89}Zr sorption on HA, as well as the stability of ^{89}Zr@HA conjugate in model biological media which will may possible to consider HA as a promising carrier for ^{89}Zr.

Experimental

Synthesis of HA nanoparticles

The synthesis of HA nanoparticles was carried out by feeding a 30% solution of orthophosphoric acid with a controlled speed (using a special peristaltic pump) into a reaction vessel with an aqueous suspension of calcium oxide/hydroxide with intensive stirring. The progress of the reaction was monitored both by the volume of the acid that had gone into the reaction (up to the stoichiometric Ca/P ratio = 1.67), and using a pH meter (Elit-3305, UK) until the reaction mixture reached a pH value of 6–7 [39]. In the resulting suspension of HA nanocrystals, the mass concentration of the solid phase (X_t, %) was determined gravimetrically, which was equal to $X_t = 5.5 \pm 0.2$ mass%.

The morphology and size characteristics of the particles of the solid phase were studied by electron transmission microscopy (JEM-1011B, Japan, resolution 0.3 nm). Transmission electron microscopy samples were prepared by applying a drop of a suspension of the studied crystals diluted with distilled water in a ratio of 50:1 on a special copper mesh with a form film. After drying in air, the samples were stored in special canisters.

The phase composition of the HA powder obtained from the initial suspension was characterized by XRD. X-ray diffraction patterns of the experimental samples were obtained using a DRON-3 automated X-ray diffractometer, focused according to Bragg-Bretano, with a graphite monochromator on a diffracted beam, controlled using the EXPRESS computer program. The measurements were carried out on a CoKα detector with the radiation wavelength of 0.179021 nm in the step-by-step scanning mode in the range of angles 10°–80° (2θ) with a step of 0.1°–0.05°; the exposure time for one point was 3–5 s.

The specific free surface and porosity were determined for the powder by thermal desorption of nitrogen (Micrometrics ASAP-2010, USA). The results were processed according to the Branauer-Emmett-Taylor (BET) model; temperature was − 196 °C and relative vapor pressure $P/P_0 = 0.2$. The pore sizes in the texture of the samples (with a diameter of < 100 nm) were determined according to the Barrett–Joyner–Halender model.

Carrier-free ^{89}Zr separation and its detection

To obtain carrier-free ^{89}Zr, two 100 mg Y_2O_3 targets were irradiated with 15 MeV deuterons and dissolved in HCl_{conc}. Then, separations by extraction chromatography on TEVA sorbent (based on quaternary ammonium salts, Triskem Int, France, 100–150 mesh) were carried out for few mg parts of targets according to our previously determined distribution coefficients and developed separation method [15] (Fig. 1). Measurements of the activity of ^{89}Zr were carried out on gamma spectrometer using 909 keV (100%) peak. For this, gamma spectrometer with a high-purity germanium detector GR 3818 (Canberra Inc, USA) calibrated by certified reference point sources (^{22}Na, ^{60}Co, ^{241}Am and ^{137}Cs) and a ^{152}Eu standard solution was used.

^{89}Zr sorption on HA nanoparticles

For sorption experiments a suspension of HA 5.5 mass% and previously obtained carrier-free ^{89}Zr solution were

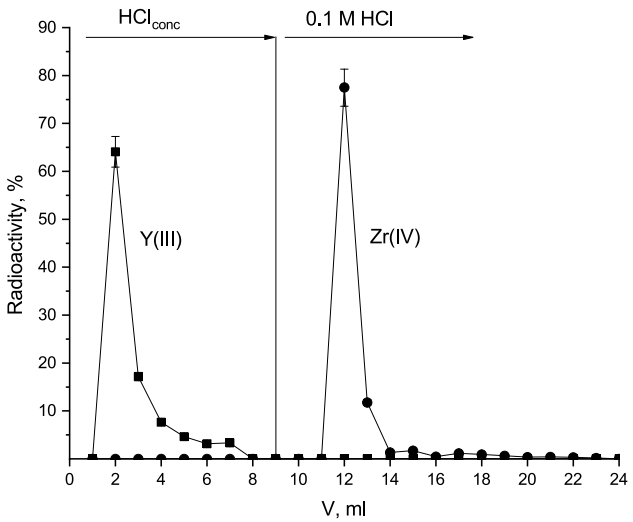

Fig. 1 Separation of carrier-free ^{89}Zr from target material onto TEVA resin. Column had 2 ml volume and 7 mm diameter

used. Temperature of 25 °C was kept during all sorption experiments.

To study the interaction parameters of ultramicroquantities of Zr(IV) with the surface of the sorbent, an adsorption isotherm was constructed. For this, the sorption values were studied at various concentrations of Zr(IV) with fixed HA content in solution (0.55 mass%). The amount of zirconium was from the minimum detectable activity under measurement conditions (300 Bq per experiment) to 10^{-8} g (by adding a stable Zr(IV) carrier to solution up to mass equivalent of 150 MBq of ^{89}Zr).

To study influence of pH to ^{89}Zr sorption, a 1 ml suspension of HA was placed in a 10 ml plastic vial, a solution of selected for sorption medium was added, then an aliquot of the $ZrOCl_2 \cdot 8H_2O$ solution (the total content of stable zirconium in this solution was 10^{-8} g, which is equivalent to 150 MBq ^{89}Zr and exceeds the medical dose), and finally, an aliquot of ^{89}Zr solution. After a few minutes, the pH of the solution was measured. The contents of the vial were then mixed on a shaker, centrifuged, an aliquot of the solution was taken, and the gamma spectrum was registered.

In all further experiments with fixed pH the amount of all reagents except stable zirconium (carrier) was reduced by 10 times and experiments were carried out in eppendorf test tubes with total volume of 1 mL.

To determine the amount of desorption, sorption was carried out in 1 mL of solution, then, after 15 min of shaking, the solution was centrifuged and 0.9 mL of solution was removed. Then, 0.9 mL of bovine serum albumin (BSA) in phosphate-buffered saline with pH 7.3 (PBS) was added to the supernatant and suspension remaining in the test tube, so that the concentration of BSA after addition was 40 g/L. Finally, the resulting solution was agitated, shaken at 37 °C, an aliquot was taken and the gamma spectrum was registered.

For each sorption and desorption values, 3 parallel experiments were performed.

Results and discussion

Characterization of HA nanoparticles

As a result of the synthesis of HA, an aqueous suspension of its nanocrystals (white) with a solid phase content of $X_m = 5.5 \pm 0.2$ mass was obtained. According to electron transmission microscopy, HA nanoparticles are elongated plate crystals with an average size of 100–25 nm (length–width) and a thickness of about 2–5 nm. According to the work [40] the thickness of an individual HA nanocrystal can reach a value comparable to the unit cell size of the HA itself (0.6–0.8 nm). Nanoplates in suspension are assembled into aggregates with a complex hierarchical organization (Fig. 2).

According to the XRD data, only HA reflexes are present in the diffractogram of the experimental samples (Fig. 3). The broadening of reflections on the diffractogram is associated precisely with the nanodispersity of the drug.

The specific free surface of the solid sample was about 80 m^2/g. In this case, the maximum surface of HA nanoparticles, indirectly determined in collagen sorption experiments or calculated from the geometrical dimensions of the hydroxyapatite [40] is at the level of 900 m^2/g. Taking into account the degree of aggregation of nanoparticles, we estimate the specific free surface of the HA as 180-200 m^2/g.

Sorption behavior of ^{89}Zr on HA nanoparticles

To determine the optimal conditions for ^{89}Zr sorption on HA, experiments were carried out in distilled water at various pH by adding an aliquot of HCl or NaOH. It was found that in the entire selected pH range, sorption is close to quantitative and amounts to more than 98.5% (Fig. 4).

To study the effect of the ionic strength of the solution, sorption experiments were also carried out in a 0.9% NaCl solution at the same pH values, as a result of which it was found that the sorption value does not change in comparison with sorption in water.

To construct the isotherm of sorption of zirconium on HA, low concentrations were chosen so as not to significantly exceed the medical amount of ^{89}Zr. As expected, in this case, sorption is described by the Henry isotherm (Fig. 5), while the experimentally determined Henry constant was 0.35 ± 0.02 L/g. The data obtained indicate the

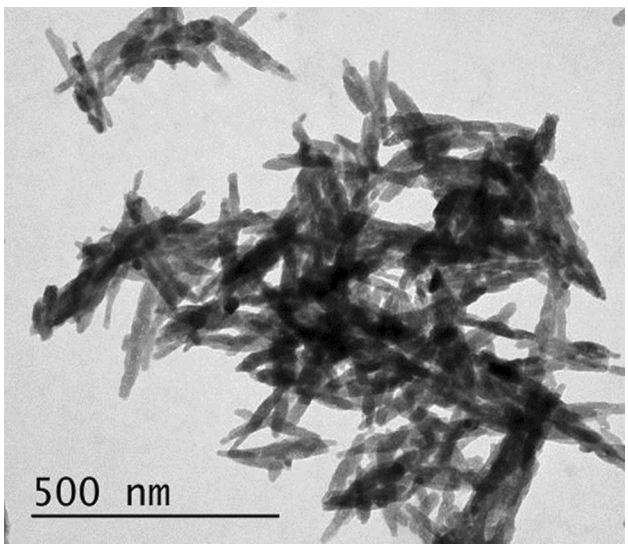

Fig. 2 Morphology of HA nanocrystals

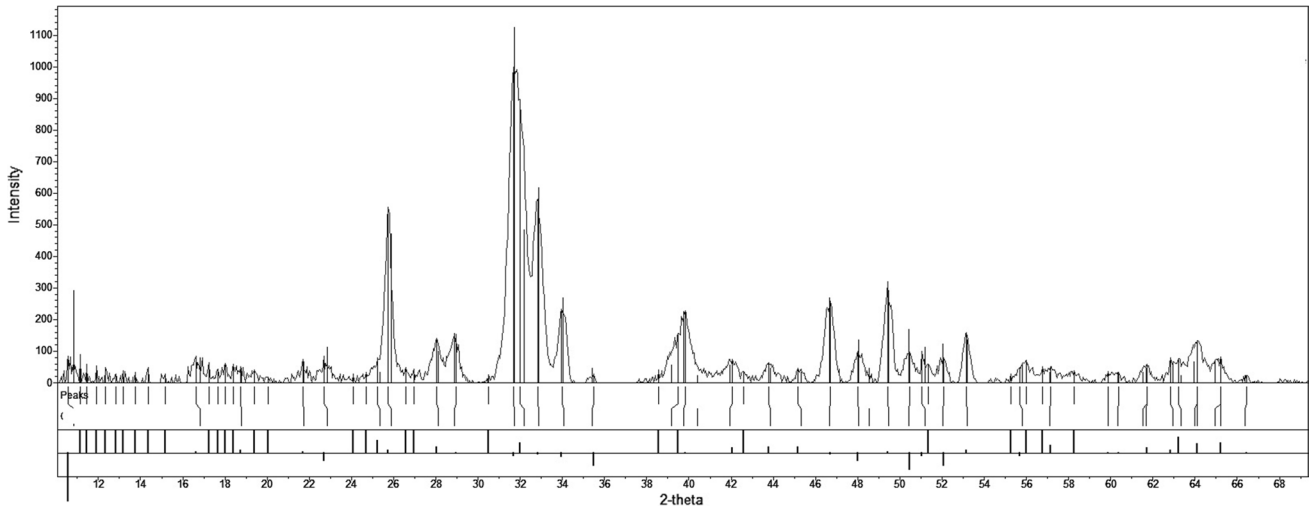

Fig. 3 Experimental X-ray diffraction pattern of HA and HA reference lines according to the JCPDS catalog

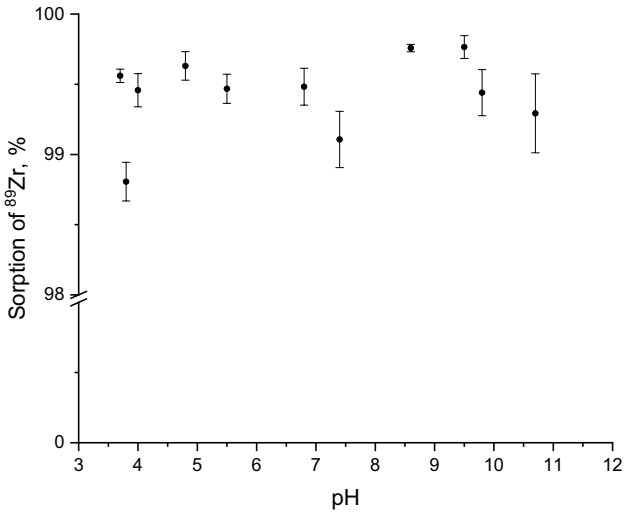

Fig. 4 Sorption of ^{89}Zr on HA nanoparticles (0.55 mass%) in an aqueous medium with addition of HCl or NaOH at 25 °C

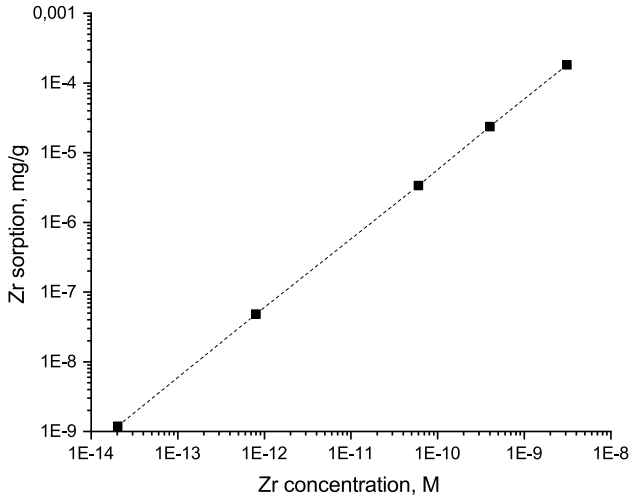

Fig. 5 Sorption isotherm of Zr(IV) on HA nanoparticles for low Zr(IV) concentrations in water solutions with pH 7

possibility of using small amounts of HA for the complete sorption of ^{89}Zr medical quantities.

A study of the kinetics of the sorption process (from 3 to 30 min of sorption at pH 4, 7, and 10) showed that sorption equilibrium in both media is achieved in the first minutes of contact of HA and ^{89}Zr (Fig. 6).

Next, the effect of the amount of HA on sorption at pH 7.3 (adding sodium acetate to the solution to maintain an appropriate pH) was studied. It was found that in the investigated range of HA content in the solution from 0.055 to 1.1 mass%, the sorption value does not change. Thus, sorption of ^{89}Zr on HA can be carried out in a wide range of pH and HA concentrations, while complete sorption of ^{89}Zr by nanoparticles in all cases will be achieved in just a few minutes.

Finally, the desorption of ^{89}Zr in a 40 g/L BSA solution in PBS (a solution simulating both ionic strength and blood protein background) was studied. The contact time of ^{89}Zr@HA with a stripping solution ranged from 60 min to 2 days, and it was shown that both at 25 °C and at 37° C the desorption is minimal, and reaches only 0.6% in 2 days (Fig. 6).

Thus, the possibility of easy and quick synthesis of the ^{89}Zr@HA conjugate, which can be potentially used in various tasks in nuclear medicine, was demonstrated in the work. In addition to the direct use of the conjugate for visualization in the body, its further modification is possible. During the sorption of ultramicroquantities of ^{89}Zr, HA retains its structure and properties (which was demonstrated in our experiments by the constancy of the XRD spectrum before

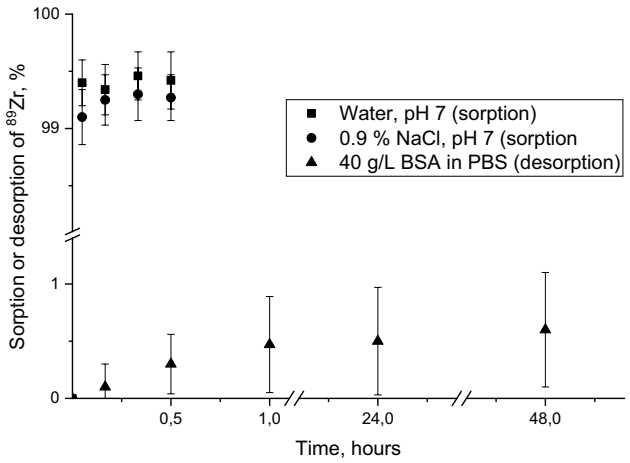

Fig. 6 Kinetics of sorption (25 °C) and desorption (37 °C) of ^{89}Zr on 0.55 mass% HA

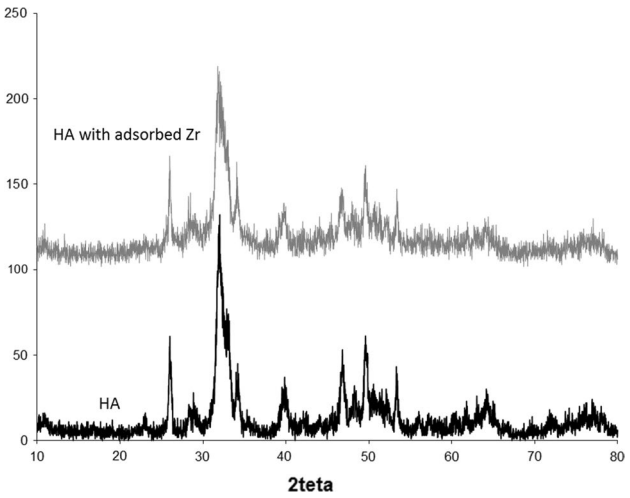

Fig. 7 XRD spectra of initial HA and HA with adsorbed Zr

and after sorption, Fig. 7), including the ability to bind to different compounds, which will subsequently allow selective synthesis of conjugates to solve various problems (by analogy with works [41–46]). The stability of the obtained conjugate to desorption also confirms the prospects for the further use of ^{89}Zr@HA and its modifications.

Conclusions

In this work, the synthesis and stability in the model biological media of the ^{89}Zr@HA conjugate were studiedThe sorption value at pH from 3 to 11 was more than 98% over the entire range. It was shown that ^{89}Zr sorption on HA both in water and in 0.9% NaCl is characterized by fast kinetics: sorption equilibrium occurs in the first minutes of contact of the sorbent with a solution containing a radionuclide. A study of ^{89}Zr desorption with HA showed that the conjugate ^{89}Zr@HA is highly stable in a model biological medium: no more than 1% ^{89}Zr is desorbed from the surface in 2 days at 37 °C. The results indicate the promise of using HA as a carrier of ^{89}Zr in nuclear medicine.

Acknowledgements This work was financially supported by Russian Foundation for Basic Research (RFBR) according to research Project No 18-33-00649 (all researches except radiometrical detections which were carried out according to state task realization of Vernadsky Institute of Geochemistry and Analytical Chemistry of the Russian Academy of Sciences, Theme No. 0137-2019-0022).

References

1. Brandt M, Cardinale J, Aulsebrook ML et al (2018) An overview of PET radiochemistry, part 2: radiometals. J Nucl Med 59:1500–1506. https://doi.org/10.2967/jnumed.117.190801
2. Holland JP, Sheh Y, Lewis JS (2009) Standardized methods for the production of high specific-activity zirconium-89. Nucl Med Biol 36:729–739. https://doi.org/10.1016/j.nucmedbio.2009.05.007
3. Severin GW, Jørgensen JT, Wiehr S et al (2015) The impact of weakly bound ^{89}Zr on preclinical studies: non-specific accumulation in solid tumors and aspergillus infection. Nucl Med Biol 42:360–368. https://doi.org/10.1016/j.nucmedbio.2014.11.005
4. Degering D, Unterricker S, Stolz W (1988) Excitation function of the ^{89}Y(d,2n)^{89}Zr reaction. J Radioanal Nucl Chem Lett 127:7–11. https://doi.org/10.1007/BF02165500
5. Ciarmatori A, Cicoria G, Pancaldi D et al (2011) Some experimental studies on ^{89}Zr production. Radiochim Acta 99:631–634. https://doi.org/10.1524/ract.2011.1822
6. Dejesus OT, Nickles RJ (1990) Production and purification of ^{89}Zr, a potential PET antibody label. Int J Radiat Appl Instrum Part 41:789–790. https://doi.org/10.1016/0883-2889(90)90030-K
7. Lahiri S, Mukhopadhyay B, Das NR (1997) Simultaneous production of ^{89}Zr and ^{90,91m,92m}Nb in α-particle activated yttrium and their subsequent separation by HDEHP. Appl Radiat Isot 48:883–886. https://doi.org/10.1016/S0969-8043(96)00338-7
8. Kandil SA, Scholten B, Saleh ZA et al (2007) A comparative study on the separation of radiozirconium via ion-exchange and solvent extraction techniques, with particular reference to the production of ^{88}Zr and ^{89}Zr in proton induced reactions on yttrium. J Radioanal Nucl Chem 274:45–52. https://doi.org/10.1007/s10967-006-6892-2
9. Kasbollah A, Eu P, Cowell S, Deb P (2013) Review on production of ^{89}Zr in a medical cyclotron for PET radiopharmaceuticals. J Nucl Med Technol 41:35–41. https://doi.org/10.2967/jnmt.112.111377
10. Meijs WE, Herscheid JDM, Haisma HJ et al (1994) Production of highly pure no-carrier added ^{89}Zr for the labelling of antibodies with a positron emitter. Appl Radiat Isot 45:1143–1147. https://doi.org/10.1016/0969-8043(94)90029-9
11. Queern SL, Aweda TA, Massicano AVF et al (2017) Production of Zr-89 using sputtered yttrium coin targets. Nucl Med Biol 50:11–16. https://doi.org/10.1016/j.nucmedbio.2017.03.004
12. Pandey MK, Engelbrecht HP, Byrne JP et al (2014) Production of 89Zr via the 89Y(p, n)89Zr reaction in aqueous solution: effect of solution composition on in-target chemistry. Nucl Med Biol 41:309–316. https://doi.org/10.1016/j.nucmedbio.2014.01.006

13. Verel I, Visser GWM, Boellaard R et al (2003) ^{89}Zr immuno-PET: comprehensive procedures for the production of ^{89}Zr-labeled monoclonal antibodies. J Nucl Med 44:1271–1281
14. Ekatova TY, Kazakov AG (2019) Extraction-chromatographic behavior of Zr(IV) and Hf(IV) on TRU and LN resins in mixtures of HNO_3 and HF. J Radioanal Nucl Chem 321:557–563. https://doi.org/10.1007/s10967-019-06601-x
15. Kazakov AG, Aliev RA, Ostapenko VS et al (2018) Separation of ^{89}Zr from irradiated yttrium targets by extraction chromatography. J Radioanal Nucl Chem 317:605–611. https://doi.org/10.1007/s10967-018-5888-z
16. Heskamp S, Raavé R, Boerman OC et al (2017) ^{89}Zr-immunoPET in oncology: state of the art ^{89}Zr-radiochemistry. Bioconjug Chem 28:2211–2223. https://doi.org/10.1021/acs.bioconjchem.7b00325
17. Heskamp S, van Laarhoven HWM, Molkenboer-Kuenen JDM et al (2010) ImmunoSPECT and immunoPET of IGF-1R expression with the radiolabeled antibody R1507 in a triple-negative breast cancer model. J Nucl Med 51:1565–1572. https://doi.org/10.2967/jnumed.110.075648
18. Perk LR, Visser OJ, Stigter-Van Walsum M et al (2006) Preparation and evaluation of ^{89}Zr-Zevalin for monitoring of ^{90}Y-Zevalin biodistribution with positron emission tomography. Eur J Nucl Med Mol Imaging 33:1337–1345. https://doi.org/10.1007/s00259-006-0160-0
19. Pandya DN, Pailloux S, Tatum D et al (2015) Di-macrocyclic terephthalamide ligands as chelators for the PET radionuclide zirconium-89. Chem Commun 51:2301–2303. https://doi.org/10.1039/C4CC09256B
20. Deri MA, Ponnala S, Zeglis BM et al (2014) Alternative chelator for ^{89}Zr radiopharmaceuticals: radiolabeling and evaluation of 3,4,3-(LI-1,2-HOPO). J Med Chem 57:4849–4860. https://doi.org/10.1021/jm500389b
21. Zhai C, Summer D, Rangger C et al (2015) Novel bifunctional cyclic chelator for ^{89}Zr labeling-radiolabeling and targeting properties of RGD conjugates. Mol Pharm 12:2142–2150. https://doi.org/10.1021/acs.molpharmaceut.5b00128
22. Deri MA, Ponnala S, Kozlowski P et al (2015) P-SCN-BN-HOPO: a superior bifunctional chelator for ^{89}Zr immunoPET. Bioconjug Chem 26:2579–2591. https://doi.org/10.1021/acs.bioconjchem.5b00572
23. Perez-Medina C, Tang J, Abdel-Atti D et al (2015) PET imaging of tumor-associated macrophages with ^{89}Zr-labeled high-density lipoprotein nanoparticles. J Nucl Med 56:1272–1277. https://doi.org/10.2967/jnumed.115.158956
24. Perez-Medina C, Abdel-Atti D, Zhang Y et al (2014) A modular labeling strategy for in vivo PET and near-infrared fluorescence imaging of nanoparticle tumor targeting. J Nucl Med 55:1706–1711. https://doi.org/10.2967/jnumed.114.141861
25. Li N, Yu Z, Pham T et al (2017) A generic ^{89}Zr labeling method to quantify the in vivo pharmacokinetics of liposomal nanoparticles with positron emission tomography. Int J Nanomed 12:3281–3294. https://doi.org/10.2147/IJN.S134379
26. Zhao Y, Shaffer TM, Das S et al (2017) Near-infrared quantum dot and ^{89}Zr dual-labeled nanoparticles for in vivo Cerenkov imaging. Bioconjug Chem 28:600–608. https://doi.org/10.1021/acs.bioconjchem.6b00687
27. Karmani L, Labar D, Valembois V et al (2013) Antibody-functionalized nanoparticles for imaging cancer: influence of conjugation to gold nanoparticles on the biodistribution of ^{89}Zr-labeled cetuximab in mice. Contrast Media Mol Imaging 8:402–408. https://doi.org/10.1002/cmmi.1539
28. Cheng L, Kamkaew A, Shen S et al (2016) Facile preparation of multifunctional WS_2/WO_x nanodots for chelator-free ^{89}Zr-labeling and in vivo PET imaging. Small 12:5750–5758. https://doi.org/10.1002/smll.201601696
29. Kolmas J, Krukowski S, Laskus A, Jurkitewicz M (2016) Synthetic hydroxyapatite in pharmaceutical applications. Ceram Int 42:2472–2487. https://doi.org/10.1016/j.ceramint.2015.10.048
30. Chakraborty S, Das T, Sarma HD et al (2008) Preparation and preliminary studies on ^{177}Lu-labeled hydroxyapatite particles for possible use in the therapy of liver cancer. Nucl Med Biol 35:589–597. https://doi.org/10.1016/j.nucmedbio.2008.03.003
31. Chakraborty S, Vimalnath KV, Rajeswari A et al (2014) Preparation, evaluation, and first clinical use of ^{177}Lu-labeled hydroxyapatite (HA) particles in the treatment of rheumatoid arthritis: utility of cold kits for convenient dose formulation at hospital radiopharmacy. J Label Compd Radiopharm 57:453–462. https://doi.org/10.1002/jlcr.3202
32. Clunie G, Lui D, Cullum I et al (1995) Samarium-153-particulate hydroxyapatite radiation synovectomy: biodistribution data for chronic knee synovitis. J Nucl Med 36:51–57
33. Vasiliev AN, Severin A, Lapshina E et al (2017) Hydroxyapatite particles as carriers for ^{223}Ra. J Radioanal Nucl Chem 311:1503–1509. https://doi.org/10.1007/s10967-016-5007-y
34. Severin AV, Orlova MA, Shalamova ES et al (2019) Nanohydroxyapatite and its textures as potential carriers of promising short-lived lead isotopes. Russ Chem Bull 68:2197–2204. https://doi.org/10.1007/s11172-019-2688-8
35. Orlova MA, Nikolaev AL, Trofimova TP et al (2019) Hydroxyapatite and porphyrin-fullerene nanoparticles for diagnostic and therapeutic delivery of paramagnetic ions and radionuclides. Bull Russ State Med Univ. https://doi.org/10.24075/brsmu.2018.075
36. Orlova MA, Nikolaev AL, Trofimova TP et al (2019) Specific properties of hydroxyapatite as a potential transporter of copper ions and its complexes. Russ Chem Bull 68:1102–1108. https://doi.org/10.1007/s11172-019-2526-z
37. Teterin YA, Kazakov AG, Teterin AY et al (2019) The study of Zr adsorption on nanodispersed hydroxyapatite: X-ray photoelectron study. J Radioanal Nucl Chem 321:341–347. https://doi.org/10.1007/s10967-019-06586-7
38. Severin AV, Orlova MA, Shalamova ES et al (2017) Sorption and cytotoxicity of zinc on hydroxyapatite. Russ Chem Bull 66:9–15. https://doi.org/10.1007/s11172-017-1692-0
39. Severin AV, Pankratov DA (2016) Synthesis of nanohydroxyapatite in the presence of iron(III) ions. Russ J Inorg Chem 61:265–272. https://doi.org/10.1134/s0036023616030190
40. Melikhov IV, Komarov VF, SAV (2000) Two-dimensional crystal hydroxyapatite. Rep Russ Acad Sci 373:355 **(in Russian)**
41. Lobaz V, Konefał R, Pánek J et al (2019) In situ in vivo radiolabeling of polymer-coated hydroxyapatite nanoparticles to track their biodistribution in mice. Colloids Surf B Biointerfaces 179:143–152. https://doi.org/10.1016/j.colsurfb.2019.03.057
42. Adamiano A, Iafisco M, Sandri M et al (2018) On the use of superparamagnetic hydroxyapatite nanoparticles as an agent for magnetic and nuclear in vivo imaging. Acta Biomater 73:458–469. https://doi.org/10.1016/j.actbio.2018.04.040
43. Salek N, Bahrami-Samani A, Shirvani-Arani S et al (2018) Highly stable ^{177}Lu-organic framework as a potential agent for treatment of metastatic bone. IEEE Trans Nanobiosci 17:361–371. https://doi.org/10.1109/TNB.2018.2830812
44. Cole LE, McGinnity TL, Irimata LE et al (2018) Effects of bisphosphonate ligands and PEGylation on targeted delivery of gold nanoparticles for contrast-enhanced radiographic detection of breast microcalcifications. Acta Biomater 82:122–132. https://doi.org/10.1016/j.actbio.2018.10.014
45. Ishizaki A, Mishiro K, Shiba K et al (2019) Fundamental study of radiogallium-labeled aspartic acid peptides introducing octreotate derivatives. Ann Nucl Med 33:244–251. https://doi.org/10.1007/s12149-018-01326-5

46. Attar Nosrati S, Alizadeh R, Ahmadi SJ, Erfani M (2019) Design, synthesis and characterization of hydroxyapatite-chitosan nanocomposite radiolabelled with ^{153}Sm as radiopharmaceutical for use in radiosynovectomy. Radiochim Acta 108:57–65. https://doi.org/10.1515/ract-2018-3038